Smooth Particle Methods for Vapour Liquid Coexistence.

A. Charles[1] and P. Daivis[1]

[1] *Condensed Matter Theory Group, School of Applied Science, RMIT University.*
Email: a.charles@bom.gov.au

Abstract: The vapour-liquid phase transition exhibits remarkable complexity and requires sophisticated modeling to explain in detail.

The complex structure of a condensing quenched vapour suggests Lagrangian particle methods like smoothed particle hydrodynamics (SPH), smooth particle applied mechanics (SPAM) and dissipative particle dynamics (DPD) as natural numerical techniques. Lagrangian particle methods allow for arbitrarily complex flows, do not suffer from mesh tangling and avoid unstable modes associated with grid methods. Mesoscopic, coarse grained models of phase transitions are of current interest because of their potential applications to the fabrication of microstructures.

In smooth particle methods the fluid is represented as a set of particles that carry the properties of the fluid and interact according to equations of motion that are derived in a clear and consistent way from the continuum equations and constitutive relations for the system. We see this as an advantage over lattice methods in which the relationship between the model dynamics and the continuum equations is less clear.

We have developed a high performance smooth particle code for modeling small systems of the order of 1000s of particles. The code is built flexibly to allow for experimentation with the form of the smooth particle equations and the various parameters. Lagrangian particle methods do bring their own set of numerical challenges, most of which have straightforward numerical corrections. Our code incorporates many of these well understood corrections including artificial viscosity and anti-clumping measures. Our technique is closely related to modern implementations of DPD with a key difference that we do not explicitly model thermal fluctuations.

By solving the equations of motion for a mean-field van der Waals equation of state we are able to produce droplets, bubbles and planar gas-liquid interfaces under a variety of boundary conditions. Surface tension arises through the attractive part of the van der Waals equation of state and the van der Waals square gradient term. As scale decreases the capillary terms, which are driven by density gradients, become more important to the dynamics of the phase separating fluid.

We do not need to use different particle types or different equations of state to represent the two phases. Instead the phase separation of the one component fluid arises naturally out of the van der Waals model. No explicit tracking of the vapour-liquid interface is required.

To produce sensible results we need to ensure the cohesive pressure operates at a longer range than the repulsive pressure. We do not yet understand if this is required for consistency with mean-field theory, or is needed purely for numerical stability.

Quenching a supercritical gas in a long periodic box we are able to realise the interconnected domains characteristic of spinodal decomposition, with indications that short time liquid-gas domain growth and long time hydrodynamic domain coalescence are correctly captured. Phase separating systems equilibrate to domains of coexisting vapour and liquid at the expected densities for the van der Waals model.

Our method and code shows qualitative ability and quantitative promise. It is ready to be tested against real experimental data, under more complex boundary conditions and against more complicated phase diagrams involving more than one component. The smooth particle framework we have used can be naturally extended to handle concentration gradients, arbitrary boundary conditions, and other equations of state.

Keywords: Smooth particle, van der Waals, phase separation, condensation

1. CONDENSATION

The van der Waals equation of state provides a simple, elegant model for the coexistence of vapour and liquid. It is based on the assumption of a long range mean field attraction a between molecules and a hard core excluded volume b, and gives the pressure p as a function of number density n and temperature T (van Kampen, 1964):

$$p = \frac{n k_b T}{1 - nb} - an^2. \tag{1}$$
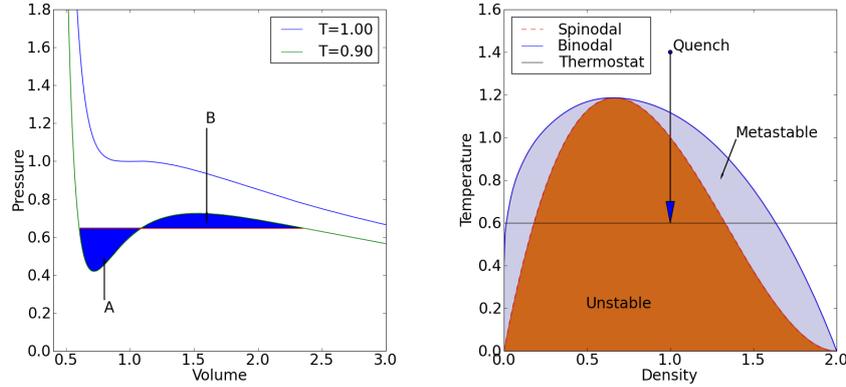
Figure 1: Left: The van der Waals equation of state, with the Maxwell construction tie line. Right: The phase diagram in the temperature density plane for a quenched one component van der Waals fluid.

The kink in the equation of state below the critical point is called a van der Waals loop. In this region the system prefers to separate into two phases such that the overall free energy (given by the area under the pressure-volume curve) is minimised. This phase separation is represented as a constant pressure line on the equation of state known as the Maxwell construction where areas A and B shown in figure 1 are equal. The binodal line consists of points created in this manner and bounds the region where a vapour and liquid phase coexist.

Figure 1 right shows the region of two phase coexistence. In the mechanically unstable spinodal region the derivative $\frac{\partial p}{\partial \rho}$ is negative. Here the system is subject to spontaneous phase separation for infinitesimal fluctuations. The metastable region between the spinodal and binodal is stable under small fluctuations, but will phase separate subject to large enough fluctuations. When we quench our smooth particle model of an equilbrated gas to below the critical temperature into the unstable region we expect to see it phase separate.

We write the equation of state (2) in terms of the mass density ρ by introducing the parameters $\bar{a} = a/m^2$, $\bar{b} = b/m$ and $\bar{k}_b = k_b/m$ where m is the molecular mass and $\rho = mn$.

$$p = \frac{\rho \bar{k}_b T}{1 - \rho \bar{b}} - \bar{a} \rho^2 \tag{2}$$

Following Nugent and Posch (2000) we set $\bar{a} = 2.0$, $\bar{b} = 0.5$ and $\bar{k}_b = 1$. In these units the critical temperature $T_c \approx 1.2$.

2. THE VAPOUR-LIQUID INTERFACE

The vapour-liquid interface is modelled as a diffuse region where the density varies smoothly between the bulk liquid and vapour densities. Following van der Waals (1979) we use a density gradient term involving the square of the density gradient for the energy required to form and maintain density inhomogeneities. The contribution of this gradient term to the pressure tensor is given by

$$\mathbf{C} = -M \left(\rho \nabla^2 \rho + \frac{1}{2} |\nabla \rho|^2 \right) \mathbf{1} + M \nabla \rho \nabla \rho \tag{3}$$

with gradient coefficient M (Anderson et al., 1998) (Onuki, 2007). The effect of this term is to minimise density gradients by imposing an energy penalty. Felderhof (1970) used the van der Waals square gradient theory to derive an expression for the profile of an equilibrium planar interface perpendicular to coordinate z in the vicinity of the critical point:

$$\rho(z) = \frac{1}{2}(\rho_l + \rho_g) - \frac{1}{2}(\rho_l - \rho_g)\tanh\left(\frac{\kappa z}{2}\right) \tag{4}$$

with

$$\kappa = \left(2kM^{-1}(\rho_l - \rho_g)^2\right)^{\frac{1}{2}} \tag{5}$$

where k is another constant and ρ_l ρ_g are the bulk densities of the liquid and gas phases. This density profile is shown in figure 2. The width of the interface increases with M from an infinitely thin interface with $M = 0$. In this work we use $M = 1$ for convenience. For more quantitative work molecular dynamics simulations could be used to determine the values of M and k for specific fluids. Van der Waals (1979) gives an expression for the surface tension γ of an equilibrium interfacial profile as

$$\gamma = M \int \left(\frac{d\rho(z)}{dz}\right)^2 dz. \tag{6}$$

As the critical temperature is approached the density profile becomes flatter and the integral in equation 6, and thus the surface tension, approaches zero.
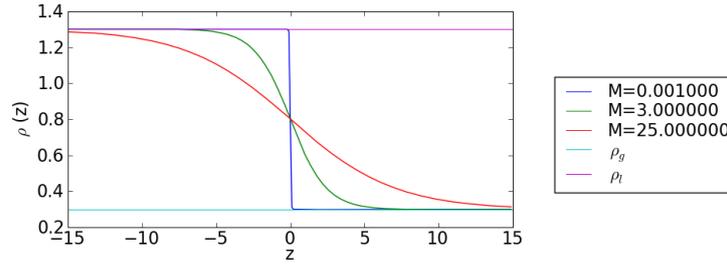
Figure 2: The liquid vapour interface in the square gradient model. The width of the interface increases with M.

3.   CONTINUUM MECHANICS

We use the van der Waals equation of state to close the Lagrangian equations of continuum mechanics which give the time rates of change of density, velocity and specific internal energy u in terms of local field variables:

$$\frac{d\rho}{dt} = -\rho \nabla \cdot \mathbf{v} \tag{7}$$

$$\frac{d\mathbf{v}}{dt} = -\frac{1}{\rho} \nabla \cdot \mathbf{P} \tag{8}$$

$$\frac{du}{dt} = \frac{1}{\rho}\left(-\nabla \cdot \mathbf{J}_q - \mathbf{P}^{\mathsf{T}} : \nabla \mathbf{v}\right) \tag{9}$$

with velocity $\mathbf{v}$. The detailed physics is in the pressure tensor $\mathbf{P}$. The heat flux given by Fourier's law $\mathbf{J}_q = -\lambda \nabla T$. We have included contributions from the equilibrium isotropic pressure determined by the equation of state, Newtonian viscosity with shear and bulk coefficients η and η_v and the the density gradient contribution C, where $(\nabla \mathbf{v})^{os}$ is the symmetric traceless velocity gradient:

$$\mathbf{P} = \left(\frac{\rho \bar{k_b} T}{1 - \rho \bar{b}} - \bar{a} \rho^2 \right) \mathbf{1} - 2\eta \left(\nabla \mathbf{v} \right)^{os} - \left(\eta_v \nabla \cdot \mathbf{v} \right) \mathbf{1} + \mathbf{C}, \tag{10}$$

with temperature given by the equilibrium equation of state

$$T = \frac{u + a\rho}{k_b}. \tag{11}$$

4. SMOOTH PARTICLE MODEL OF A VAN DER WAALS SYSTEM

Smoothed particle hydrodynamics (SPH) is a numerical technique for solving partial differential equations (PDEs) in continuum mechanics, developed by Monaghan and Gingold (1977) for astrophysical modelling. It is also known as SPAM (Smoothed Particle Applied Mechanics) in its applications to computational statistical mechanics (Hoover, 2006).

In the smooth particle method field variables are mapped by a set of arbitrarily distributed particles with macroscopic attributes including density, mass, velocity and temperature. Particle properties are smoothed over space by an interpolation kernel and particles move with the fluid's local velocity. The mathematical basis for the method is the approximation of an integral for field variable $\mathbf{f}$

$$\mathbf{f}(\mathbf{r}) = \int \mathbf{f}(\mathbf{r}')\delta(\mathbf{r} - \mathbf{r}')d\mathbf{r}' \tag{12}$$

with a density dependent weighted kernel summation over particles

$$f(\hat{\mathbf{r}}) = \sum_{i=1}^{N} \mathbf{f_i} \frac{m_i}{\rho_i} W(\mathbf{r} - \mathbf{r_i}, h) \tag{13}$$

where ρ_i and m_i are the density and mass of particle i. The smoothing kernel W is usually a cubic spline of Gaussian shape. This weighted summation is used to recover the field variables at any point in space as shown in figure 3.

Particle equations of motion are derived using this integral approximation of the continuum equations. Because the particles move with the streaming velocity of the fluid we are able to use the less complicated Lagrangian formulation of the continuum equations. The partial differential equations (PDEs) of continuum mechanics are transformed into a set of ordinary differential equations (ODEs) governing the motion of particles:

$$\rho(\mathbf{r_i}) = \sum_{j=1}^{N} m_j W(\mathbf{r_i} - \mathbf{r_j}, h) \tag{14}$$

$$\frac{d\mathbf{v_i}}{dt} = \sum_{j=1}^{N} m_j \left(\frac{\mathbf{P_j}}{\rho_i^2} + \frac{\mathbf{P_i}}{\rho_j^2} \right) \cdot \nabla_i W_{ij} \tag{15}$$
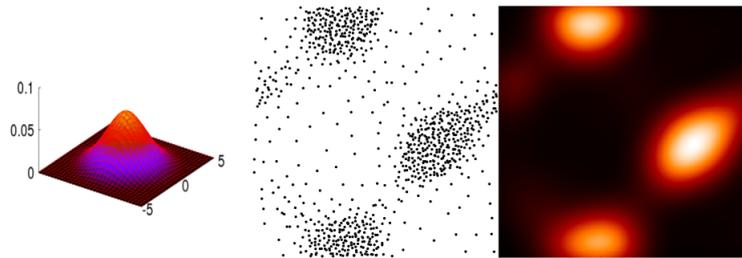
Figure 3: Left: The 'Lucy' smoothing kernel used in this work (Nugent and Posch, 2000). Centre: Particle positions. Right: Continuum smoothing of the particle plot generated using software described in Price (2007).

$$\frac{du_i}{dt} = \frac{1}{2} \sum_{j=1}^{N} m_j \left(\frac{\mathbf{P_i}}{\rho_i^2} + \frac{\mathbf{P_j}}{\rho_j^2} \right) : \mathbf{v}_{ij} \nabla_i W_{ij} - \sum_{j=1}^{N} m_j \left(\frac{\mathbf{J_{qi}}}{\rho_i^2} + \frac{\mathbf{J_{qj}}}{\rho_j^2} \right) \cdot \nabla_i W_{ij}. \tag{16}$$

Standard, symmetrised smooth particle approximations for the spatial gradients of the velocity and temperature are used (Hoover, 2006).
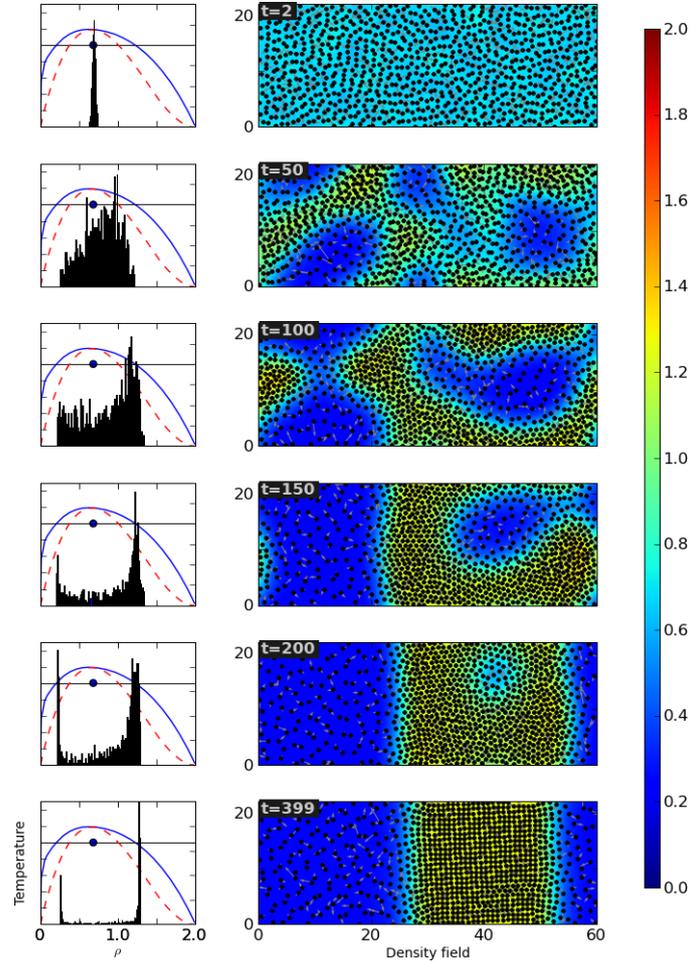
Figure 4: Condensation of a 2D smooth particle fluid. Elapsed time is denoted by t. The timestep size is 0.05. Plots on the left show the distribution of density by particle, while plots on the left show the spatially rendered mass density field. The binodal line is shown in blue. The black horizontal line shows the thermostat temperature.

5.   IMPLEMENTATION

The smooth particle algorithm is essentially the same as algorithms for classical molecular dynamics, with an additional step to compute the particle density using equation 14. Our flexible single processor Fortran 90 smoothed particle code uses a Verlet neighbour list and a fourth order Runge-Kutta integrator for timestepping to solve the equations of motion for two dimensional smooth particle systems.

To resolve stability problems when treating attractive forces we apply a longer smoothing length to the attractive component of the force between smooth particles. A similar technique is used in other particle based methods when a surface tension is required. Nugent and Posch (2000) used this method to study the formation and oscillation of liquid droplets. Hoover (2006) used an attractive density gradient force to model surface tension. Similarly in experiments with DPD, Warren (2003) enforced a density dependent interparticle potential with a long range attractive and short range repulsive central force. Tartakovsky and Meakin (2005) have used SPH to model capillary forces in fluid flow through pores by superimposing additional attractive and repulsive interparticle forces.

To prevent particle clumping we use a short range repulsive force (Hoover, 2006). To prevent the formation of ring structures and string like artefacts found by Nugent and Posch (2000) we use an adaptive smoothing length technique reported by Sigalotti et al. (2006).
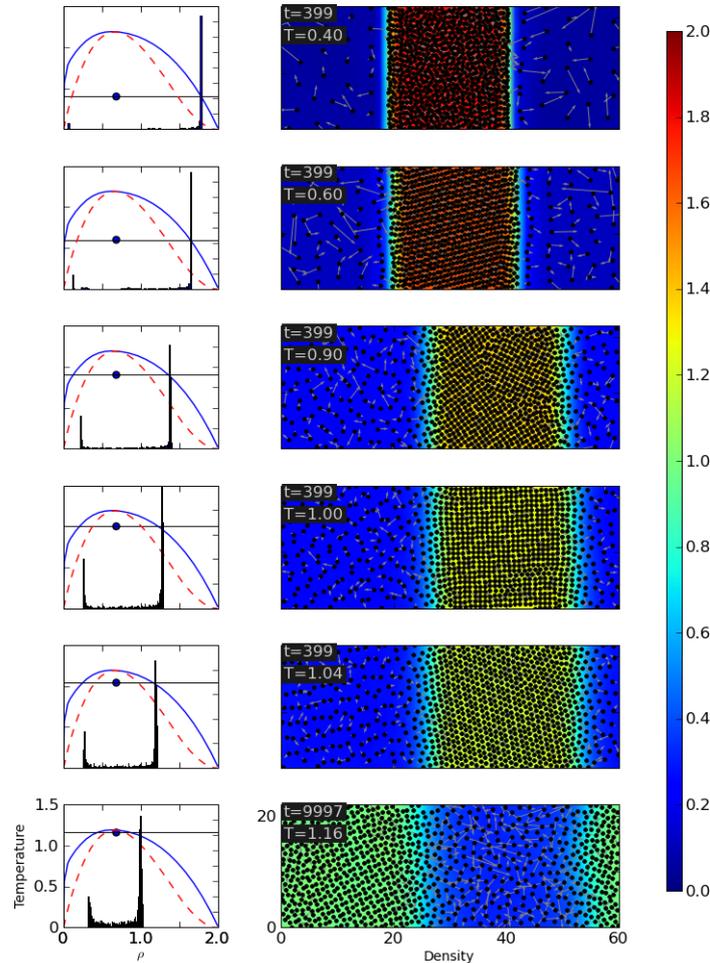
Figure 5: Coexisting vapour and liquid in equilibrium at a range of temperatures.

6.   SIMULATED CONDENSATION

Figure 4 shows the condensation of a two dimensional system in a long box with periodic boundary conditions. Initially equilibrated to a homogeneous density above the critical point, the system is quenched as shown in figure 1 and maintained at the quenched temperature using a scaling thermostat. The mass density field is rendered using the smooth particle summation (equation 14) for each pixel. The normalised distribution of particle density is overlayed on the phase diagram to show the close agreement of the final densities with predictions.

The system begins to condense in the direction of high density fluctuations (always present except for contrived cases due to the effectively random configuration of particles). Over time the domains phase separate more decisively with density peaks appearing at the expected densities. The two phase regions coalesce slowly into larger pockets and the system flows into a new configuration that minimises its surface area. The liquid density is represented quite well. We have more difficulty resolving the lowest density of the equilibrium vapour phase due to the fixed masses of the particles. Adaptive particle mass and particle splitting algorithms are being developed to solve this problem.

Figure 5 shows final equilibrium configurations for quenches at a range of temperatures. As the critical point is approached the system takes longer to phase separate.

Increasing the gradient term decreases the time to separate, and increases the interfacial width as shown in figure 6. These preliminary results exhibit the broadening of the interface predicted by theory.
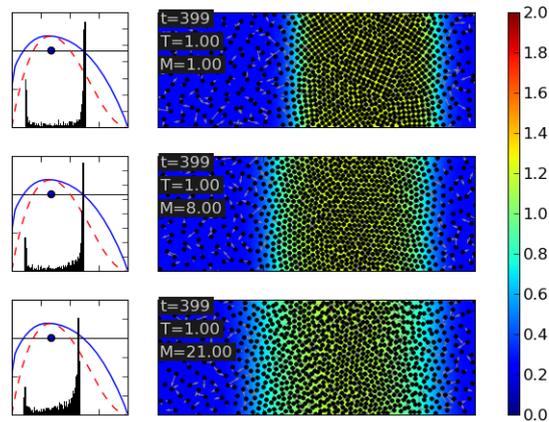
Figure 6: Vapour-liquid interfaces for different values of the gradient coefficient. Top: M = 1.0, Center: M = 8.0, Bottom: M = 21.0

7. CONCLUSION

Our smooth particle model obeys the equation of state reasonably well in the coexistence region and generates a realistic looking phase separating fluid. The interfacial width responds correctly to increases in the gradient energy coefficient, but greater resolution is needed to analyse the interfacial profile.

REFERENCES

Anderson, D. M., McFadden, G. B., and Wheeler, A. A. (1998). Diffuse-interface methods in fluid mechanics. *Annual Review of Fluid Mechanics*, 30(1):139–165.

Felderhof, B. U. (1970). Dynamics of the diffuse gas-liquid interface near the critical point. *Physica*, 48(4):541–560.

Hoover, W. G. (2006). *Smooth Particle Applied Mechanics: The State of the Art (Advanced Series in Nonlinear Dynamics)*. World Scientific Publishing Company.

Monaghan, J. J. and Gingold, R. A. (1977). Smoothed particle hydrodynamics - theory and application to non-spherical stars. *Mon. Not. R. astr. Soc.*, 181:375–389.

Nugent, S. and Posch, H. A. (2000). Liquid drops and surface tension with smoothed particle applied mechanics. *Physical Review E*, 62(4):4968.

Onuki, A. (2007). Dynamic van der waals theory. *Physical Review E (Statistical, Nonlinear, and Soft Matter Physics)*, 75(3):036304–15.

Price, D. J. (2007). SPLASH: an interactive visualisation tool for smoothed particle hydrodynamics simulations. *0709.0832*.

Sigalotti, L. D. G., Lopez, H., Donoso, A., Sira, E., and Klapp, J. (2006). A shock-capturing SPH scheme based on adaptive kernel estimation. *Journal of Computational Physics*, 212(1):124–149.

Tartakovsky, A. and Meakin, P. (2005). Modeling of surface tension and contact angles with smoothed particle hydrodynamics. *Physical Review E (Statistical, Nonlinear, and Soft Matter Physics)*, 72(2):026301–9.

van der Waals, J. D. (1979). The thermodynamic theory of capillarity under the hypothesis of a continuous variation of density. *Journal of Statistical Physics*, 20(2):200–244.

van Kampen, N. G. (1964). Condensation of a classical gas with Long-Range attraction. *Physical Review*, 135(2A):A362.

Warren, P. B. (2003). Vapor-liquid coexistence in many-body dissipative particle dynamics. *Physical Review E*, 68(6):066702.